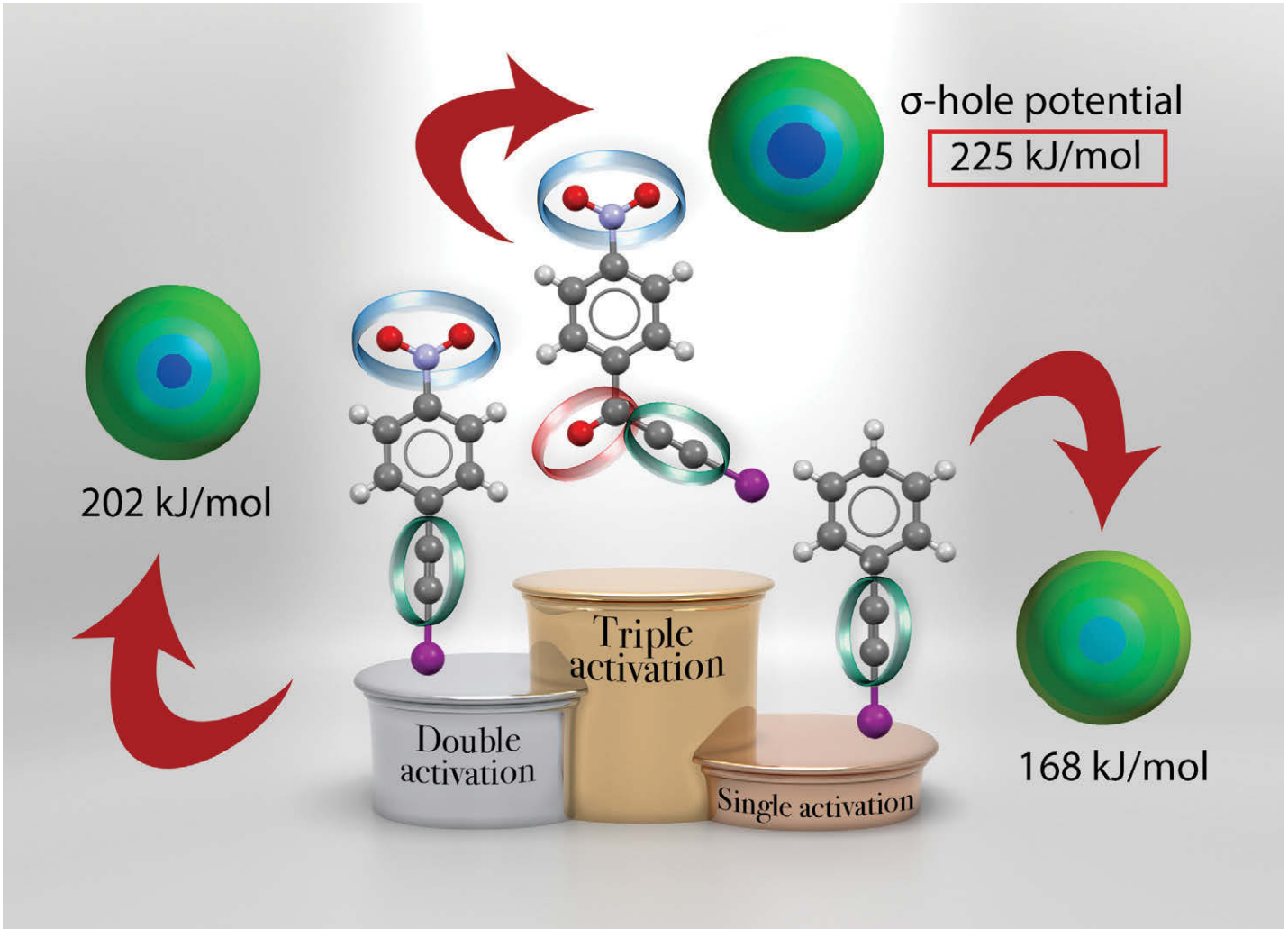


**Showcasing research from Professor Aakeröy's laboratory, Department of Chemistry, Kansas State University, Manhattan, KS, USA.**

A family of powerful halogen-bond donors: a structural and theoretical analysis of triply activated 3-iodo-1-phenylprop-2-yn-1-ones

A new class of triply-activated halogen-bond donors have been developed using structural and theoretical tools. These 3-iodo-1-phenylprop-2-yn-1-ones demonstrate several features that make them promising additions to the crystal engineering tool-box for the bottom-up assembly of functional materials with specific architectures.

## As featured in:

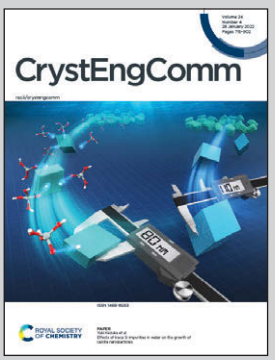


See Christer B. Aakeröy *et al.*, *CrystEngComm*, 2022, **24**, 738.

ROYAL SOCIETY OF CHEMISTRY

rsc.li/crystengcomm

Registered charity number: 207890

CrystEngComm

ROYAL SOCIETY OF CHEMISTRY

COMMUNICATION



Cite this: *CrystEngComm*, 2022, **24**, 738

Received 26th November 2021,
Accepted 20th December 2021

DOI: 10.1039/d1ce01583d

rsc.li/crystengcomm

# A family of powerful halogen-bond donors: a structural and theoretical analysis of triply activated 3-iodo-1-phenylprop-2-yn-1-ones†

Vinu V. Panikkattu, Abhijeet S. Sinha and Christer B. Aakeröy *

**Strong halogen bonds can provide a foundation for reliable supramolecular strategies for effective self-assembly and design of functional materials. A new class of halogen-bond donors have been developed using structural and theoretical tools and these 3-iodo-1-phenylprop-2-yn-1-ones demonstrate several features that make them promising additions to the crystal engineering tool-box.**

Halogen bonds (XB), which fall under the umbrella of "σ-hole interactions" are often described as an attractive force between the electrophilic region on a halogen atom located along the extension of its covalent bond, and a nucleophilic region on the same or a different molecular entity.[2] Although known for decades,[4] the halogen bond has only relatively recently been recognized as a key synthetic driver in a wide range of applications involving *e.g.* liquid crystalline,[6] phosphorescent,[7] non-linear optical[8] and functional materials,[9,10] medicinal chemistry[11] and crystal engineering.[12] The structural importance of halogen bonds can be ascribed to high directionality, tunability and strength, which can be rationalized by the anisotropic molecular electrostatic potential (MEP) distribution around the halogen atom. The magnitude of the positive σ-hole potential is often used as a qualitative yardstick to assess the halogen-bond donor ability; the larger the positive value, the stronger the bond.[13] A more reliable interaction results in synthon robustness, which facilitates molecular recognition,[14] structural prediction[15] and self-assembly,[16] which are key features for effective and selective binding in biological systems.[17] In order to develop new materials that require specific structural properties that rely on directional intermolecular interactions, it is essential that we identify new halogen-bond donors capable of forming robust non-covalent interactions.

'Activation' of a halogen-bond donor with an electron withdrawing group (EWG) has been widely employed to reduce the electron density at the σ-hole and thus strengthen the resultant halogen bond.[18,19] The halogen atom can also be activated by attaching it to an sp-hybridized carbon atom which facilitates polarization and enhances the σ-hole potential further.[20–22] However, there are relatively few examples of a combination of both electron-withdrawing groups and polarization through an sp-hybridized carbon atom in order to affect 'doubly activated' halogen-bond donors.[5,23]

In the work presented herein, we demonstrate how a new class of exceptional halogen-bond donors can be synthesized by combining three different electron withdrawing moieties in parallel to affect a 'triply activated' σ-hole. The step-wise progression is illustrated in Scheme 1 where we show how the positive electrostatic potential on the iodine atom increases from 95 kJ mol$^{-1}$ on iodobenzene, by introducing an sp-hybridized carbon atom (168 kJ mol$^{-1}$),[24,25] an EWG ketone adjacent to the C≡C bond (199 kJ mol$^{-1}$), and finally another EWG on the aromatic backbone (225 kJ mol$^{-1}$).

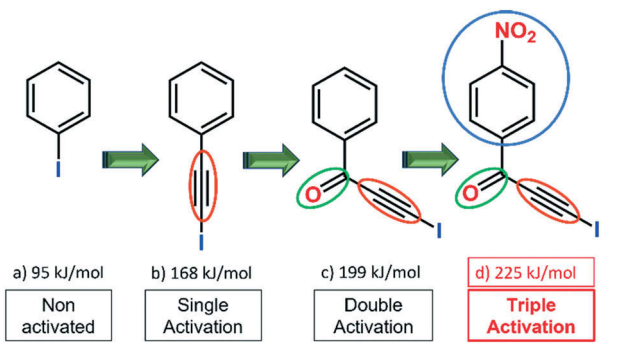


**Scheme 1** Design strategy employed in creating the library of triply activated XB donors, showing the σ-hole potentials on the iodine atom computed using DFT at B3LYP/6-311++G** level of theory at iso = 0.002.

*Department of Chemistry, Kansas State University, Manhattan, Kansas 66506, USA. E-mail: aakeroy@ksu.edu*

† Electronic supplementary information (ESI) available. CCDC numbers 2110111 (**US**), 2110113 (**4F**), 2110114 (**3CN**), 2110094 (**4CN**), 2110098 (**3N**), 2110093 (**4N**). Theoretical calculations, synthetic procedures, spectral data and crystallographic information table. For ESI and crystallographic data in CIF or other electronic format see DOI: 10.1039/d1ce01583d

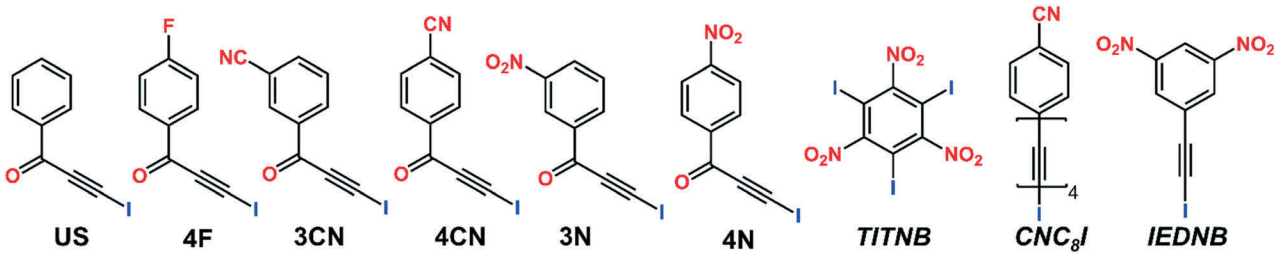


**Fig. 1** Library of target molecules explored in this study, along with the benchmark molecules from literature ***TITNB***,[1] ***CNC$_8$I***[3] & ***IEDNB***.[5]

This value is among the very highest σ-hole potentials that have been reported to date, exceeding those displayed by 'doubly activated' molecules such as 1-(iodoethynyl)-3,5-dinitrobenzene (***IEDNB***, 217.7 kJ mol$^{-1}$),[5] 4-(iodoocta-1,3,5,7-tetrayn-1-yl) benzonitrile (***CNC$_8$I***, 208.4 kJ mol$^{-1}$)[3,26] and 1,3,5-triiodo-2,4,6-trinitrobenzene (***TITNB***, 207.0).[1] The triply activated molecule offers additional synthetic scope as compared to ***TITNB***, since the aromatic backbone can be further functionalized thereby allowing us to 'dial-in' the resulting σ-hole potential and, thus, halogen-bond (XB) donor capabilities.

In this study we focus our attention on five triply activated alkyne–ketones: 4-fluoro (**4F**), 3-cyano (**3CN**), 4-cyano (**4CN**), 3-nitro (**3N**) and 4-nitro (**4N**) targets (Fig. 1). We benchmark our results against the unsubstituted parent (**US**), as well as to previously reported molecules ***TITNB***,[1] ***CNC$_8$I***[3] and ***IEDNB***,[5] which were the top performers in their respective studies.

Molecular electrostatic potential surfaces were first generated using Spartan '14 software package at the B3LYP/6-311++G** level of theory and iso = 0.002 for all molecules explored in this study (Fig. 2). σ-Hole potentials on the iodine atoms increased as follows: **US** < **4F** < ***TITNB*** < ***CNC$_8$I*** < ***IEDNB*** < **3CN** < **4CN** < **3N** < **4N**. In order to evaluate how this σ-hole potential and the relative differences between different EWG's affect the XB donor ability of the iodine atom, counterpoise (CP) corrected interaction energies (IE) were calculated between these targets and ammonia as a model acceptor at MP2/6-311++G** level of theory. I···NH$_3$ halogen bond distances for these optimized dimers were obtained and compared with the respective reduction in their combined van der Waals (vdW) radii[27] (Table 1).

The results, Table 1, indicate the that lowest σ-hole potential and IE belong to **US**, whereas the 4-nitro species (**4N**) shows the largest values among the alkyne–ketones. There is a linear relation between computed σ-hole potentials and IE with ammonia, with ***TITNB*** being the sole outlier with a much higher IE than expected, Fig. 3. In short, there is a generally excellent correlation between computed σ-hole

**Table 1** σ-Hole potential computed at B3LYP/6-311++G** at iso = 0.002 and counterpoise corrected interaction energies and halogen bond distances for dimers with ammonia computed at MP2/6-311++G**

| | σ-Hole potential | Interaction energy | Calculated XB distance | |
|---|---|---|---|---|
| Target | kJ mol$^{-1}$ | kcal mol$^{-1}$ | Å | % vdW reduction |
| **US** | 199.3 | −5.33 | 3.04 | 14.0 |
| **4F** | 206.9 | −5.49 | 3.03 | 14.2 |
| **3CN** | 221.3 | −5.84 | 3.01 | 14.6 |
| **4CN** | 222.0 | −5.85 | 3.01 | 14.7 |
| **3N** | 224.1 | −5.87 | 3.01 | 14.7 |
| **4N** | 225.2 | −5.90 | 3.01 | 14.8 |
| ***TITNB***[1] | 207.0 | −6.50 | 2.93 | 16.9 |
| ***CNC$_8$I***[3] | 210.5 | −5.57 | 3.02 | 14.5 |
| ***IEDNB***[5] | 217.7 | −5.73 | 3.01 | 14.6 |

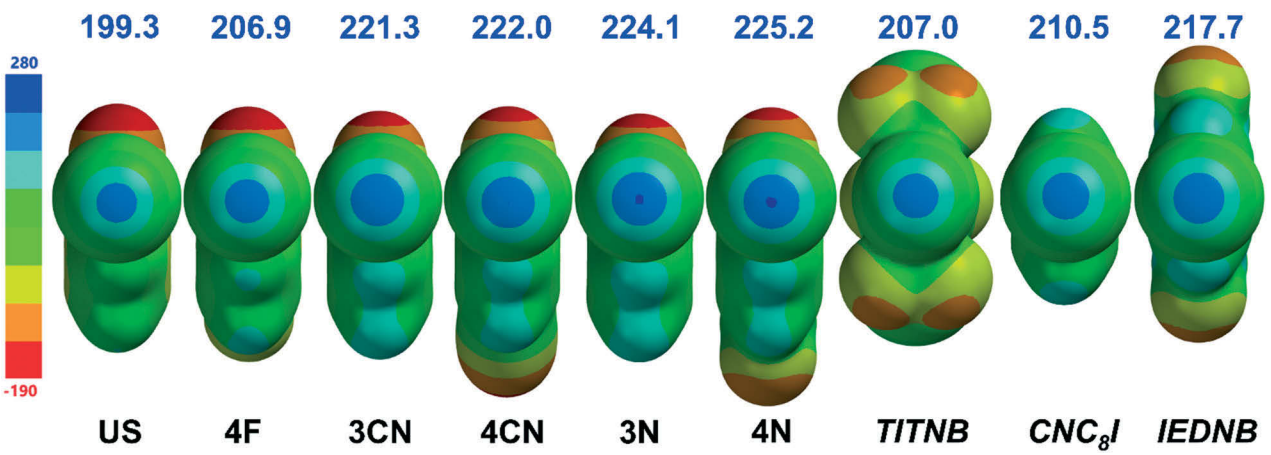


**Fig. 2** MEP surface computed at B3LYP/6-311++G** level of theory at iso = 0.002 showing σ-hole potential (top, in kJ mol$^{-1}$) on the iodine atoms of targets and benchmark compounds ***TITNB***,[1] ***CNC$_8$I***[3] and ***IEDNB***[5] explored in this study.

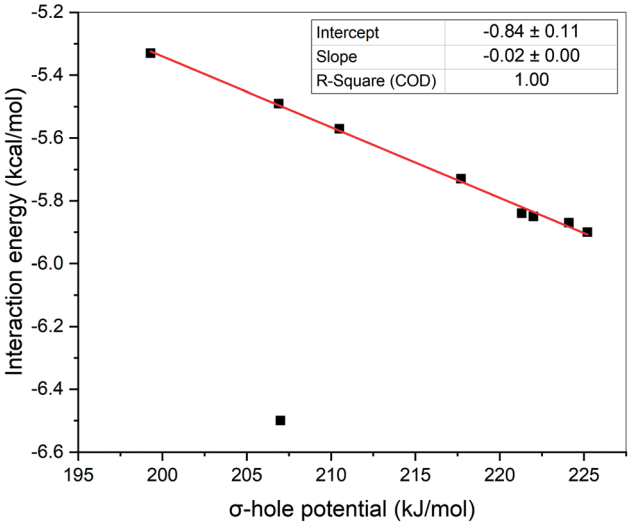


**Fig. 3** Plot of CP corrected IE *vs.* σ-hole potential for molecules explored in this study. ***TITNB***[1] outlier is excluded from the line of best fit. IE computed at MP2/6-311++G** and σ-hole potential computed at B3LYP/6-311G++G** at iso = 0.002.

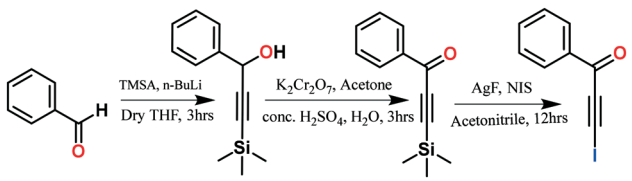


**Scheme 2** General approach for the synthesis of the targets explored in this study.

potential and increasing interaction energy. This trend is also reflected in the % reduction in the computed combined vdW radii for these halogen bonds (Table 1).

The targets were subsequently synthesized using modified versions of previously reported procedures (Scheme 2).[28–30] Detailed information along with characterization data are presented in the ESI.†

In the crystal structure of all six alkyne–ketones, there is, as expected, only one primary intermolecular interaction; the XB between the triply activated iodine atom and a suitable acceptor.

The crystal structure of **US** with only one major bond donor and acceptor, shows the expected I···O halogen bond, with a 2.887(2) Å distance and an C–I···O angle of 167.25(10)° (Fig. 4, Table 2). By adding a fluorine atom to the aromatic backbone, a 'triply activated' XB donor is produced, and the crystal structure of **4F** contains a near-linear halogen bond with a 2.836(8) Å distance and a 173.3(3)° XB angle.

The addition of cyano and nitro groups not only provides activation of the iodine XB donor, but also introduces potential XB-acceptor competitors to the C═O moiety. In fact, in the crystal structures of **3CN** and **4CN**, the C≡N moiety is shown to be the dominant acceptor site, and the resulting halogen bond is an I···N≡C interaction. In the crystal structure of **3CN**, the I···N halogen bond distance is 2.980(6) Å with a 174.06(17)° XB angle, and in **4CN** the I···N halogen bond measures 3.001(5) Å with a 169.47(19)° XB angle. The **3N** crystal structure contains two disordered molecules in the asymmetric unit, and each of those molecules have two disordered positions for the iodine atom. Yet, it is clear that the iodine atom prefers to bind to the oxygen atom of the nitro group instead of to the carbonyl group, with only one pair of iodine and oxygen atom positions among all the disordered combinations forming a I···O halogen bond measuring 2.90(3) Å and a 149.5(7)° XB angle. It is notable that this is the only dominant short contact observed in this structure apart from π–π stacking. The **4N** structure contains a bifurcated halogen bond to both oxygen atoms of the nitro group. The shorter I···O halogen bond is 3.152(3) Å with a 172.26(10)° XB angle, and the longer I···O XB measures 3.343(3) Å with a 148.21(10)° XB angle. The presence of relatively longer XB distances compared to **4N** having the

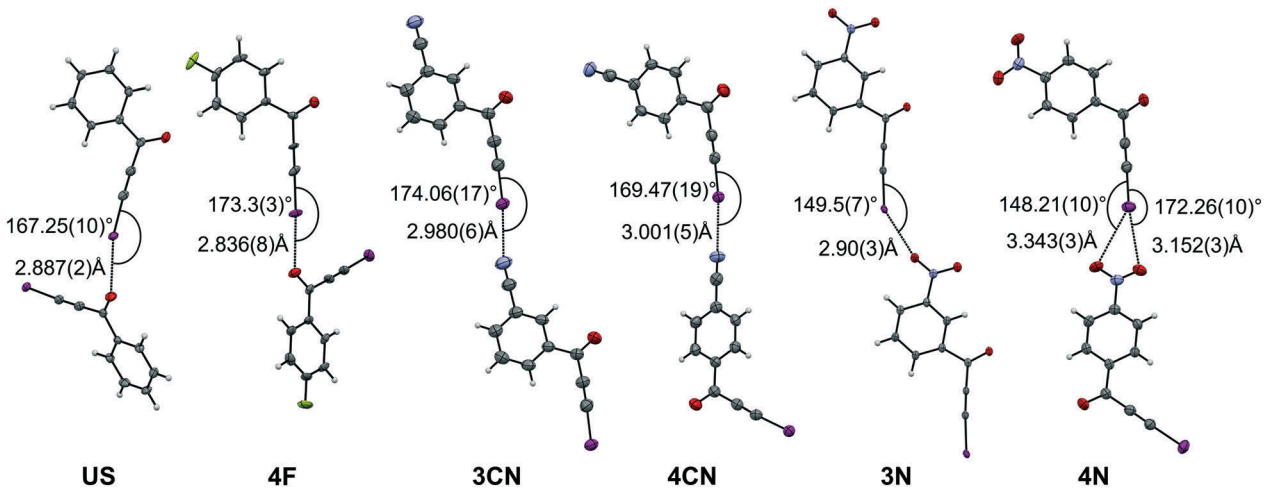


**Fig. 4** The primary halogen-bond in the crystal structures of five 'triply activated' XB donors. The unsubstituted parent (**US**) is included for comparison.

 

Table 2 σ-Hole potential computed at B3LYP/6-311++G** at iso = 0.002 and halogen bond distances and angles obtained from crystal structure

| | σ-Hole potential | Experimental XB distance | | XB angle |
|---|---|---|---|---|
| Target | kJ mol$^{-1}$ | Å | % vdW reduction | ° |
| **US** | 199.3 | 2.89 | 17.5 | 167.3 |
| **4F** | 206.9 | 2.84 | 19.0 | 173.3 |
| **3CN** | 221.3 | 2.98 | 15.6 | 174.1 |
| **4CN** | 222.0 | 3.00 | 15.0 | 169.5 |
| **3N** | 224.1 | 2.90 | 17.0 | 149.5 |
| **4N** | 225.2 | 3.15 | 9.9 | 172.3 |
| | | 3.34 | 4.6 | 148.2 |
| ***TITNB***[1] | 207.0 | 3.14 | 10.3 | 165.5 |
| ***CNC$_8$I***[3] | 210.5 | 2.89 | 18.2 | 178.5 |
| ***IEDNB***[5] | 217.7 | 3.06 | 12.6 | 168.2 |

highest σ-hole potential in our library can be attributed to the formation of a bifurcated interaction instead of a shorter and more linear single bond, a feature previously not seen in similar 4-nitro substituted molecules.[3]

In summary, through this work we have demonstrated that a combination of three different activation 'mechanisms', has a superior effect on the resulting σ-hole potential of the halogen-bond donor as compared to adding multiple EWG's of the same type, as seen by the higher σ-hole potential of **3CN**, **4CN**, **3N** and **4N** when compared to ***TITNB***[1] (possessing three nitro groups) and ***CNC$_8$I***[26] (possessing four C≡C moieties). All the triply activated targets presented herein show a high-degree of a % vdW reduction and directionality when compared to the benchmark molecules. An excellent linear correlation was observed between σ-hole potential and IE which shows that the latter can be used as a convenient and reliable yardstick when designing molecules with strong XB donors. This new family of compounds represent a new and easily accessible set of tools for the bottom-up assembly of functional co-crystals with desired and tunable metrics, and we expect that triple activation can be a broadly applied approach for the design and implementation of highly effective halogen as well as chalcogen bond donors.

## Conflicts of interest

There are no conflicts to declare.

## Acknowledgements

The authors would like to acknowledge a NOTICXE fellowship which partially funded this research. We also acknowledge the NSF-MRI grant CHE-2018414, which was used to purchase the single-crystal X-ray diffractometer and associated software employed in this study.

## Notes and references

1 N. R. Goud, O. Bolton, E. C. Burgess and A. J. Matzger, *Cryst. Growth Des.*, 2016, **16**, 1765–1771.
2 G. R. Desiraju, P. S. Ho, L. Kloo, A. C. Legon, R. Marquardt, P. Metrangolo, P. Politzer, G. Resnati and K. Rissanen, *Pure Appl. Chem.*, 2013, **85**, 1711–1713.
3 B. Pigulski, N. Gulia, P. Męcik, R. Wieczorek, A. Arendt and S. Szafert, *Cryst. Growth Des.*, 2019, **19**, 6542–6551.
4 J. M. Dumas, H. Peurichard and M. Gomel, *J. Chem. Res.*, 1978, **2**, 54–55.
5 C. B. Aakeröy, T. K. Wijethunga, J. Desper and M. Đaković, *Cryst. Growth Des.*, 2015, **15**, 3853–3861.
6 H. L. Nguyen, P. N. Horton, M. B. Hursthouse, A. C. Legon and D. W. Bruce, *J. Am. Chem. Soc.*, 2004, **126**, 16–17.
7 W. Wang, Y. Zhang and W. J. Jin, *Coord. Chem. Rev.*, 2020, **404**, 213107.
8 M. Virkki, O. Tuominen, A. Forni, M. Saccone, P. Metrangolo, G. Resnati, M. Kauranen and A. Priimagi, *J. Mater. Chem. C*, 2015, **3**, 3003–3006.
9 A. Priimagi, G. Cavallo, P. Metrangolo and G. Resnati, *Acc. Chem. Res.*, 2013, **46**, 2686–2695.
10 Z.-X. Liu, Y. Sun, Y. Feng, H. Chen, Y.-M. He and Q.-H. Fan, *Chem. Commun.*, 2016, **52**, 2269–2272.
11 R. Wilcken, M. O. Zimmermann, A. Lange, A. C. Joerger and F. M. Boeckler, *J. Med. Chem.*, 2013, **56**, 1363–1388.
12 M. C. Pfrunder, A. J. Brock, J. J. Brown, A. Grosjean, J. Ward, J. C. McMurtrie and J. K. Clegg, *Chem. Commun.*, 2018, **54**, 3974–3976.
13 T. Clark, *WIREs Comput. Mol. Sci.*, 2013, **3**, 13–20.
14 J. A. Lohrman, C.-L. Deng, T. A. Shear, L. N. Zakharov, M. M. Haley and D. W. Johnson, *Chem. Commun.*, 2019, **55**, 1919–1922.
15 A. Mukherjee, A. Sanz-Matias, G. Velpula, D. Waghray, O. Ivasenko, N. Bilbao, J. N. Harvey, K. S. Mali and S. De Feyter, *Chem. Sci.*, 2019, **10**, 3881–3891.
16 Y.-J. Zhu, Y. Gao, M.-M. Tang, J. Rebek and Y. Yu, *Chem. Commun.*, 2021, **57**, 1543–1549.
17 Z. Xu, Z. Yang, Y. Liu, Y. Lu, K. Chen and W. Zhu, *J. Chem. Inf. Model.*, 2014, **54**, 69–78.
18 P. Politzer, K. E. Riley, F. A. Bulat and J. S. Murray, *Comput. Theor. Chem.*, 2012, **998**, 2–8.
19 C. B. Aakeröy, T. K. Wijethunga and J. Desper, *J. Mol. Struct.*, 2014, **1072**, 20–27.
20 C. Perkins, S. Libri, H. Adams and L. Brammer, *CrystEngComm*, 2012, **14**, 3033–3038.
21 L. González, N. Gimeno, R. M. Tejedor, V. Polo, M. B. Ros, S. Uriel and J. L. Serrano, *Chem. Mater.*, 2013, **25**, 4503–4510.
22 C. A. Gunawardana, M. Đaković and C. B. Aakeröy, *Chem. Commun.*, 2018, **54**, 607–610.
23 J. Lieffrig, O. Jeannin and M. Fourmigué, *J. Am. Chem. Soc.*, 2013, **135**, 6200–6210.
24 R. H. Baughman, *J. Org. Chem.*, 1964, **29**, 964–965.
25 Y. V. Torubaev, K. A. Lyssenko, P. Y. Barzilovich, G. A. Saratov, M. M. Shaikh, A. Singh and P. Mathur, *CrystEngComm*, 2017, **19**, 5114–5121.
26 B. Pigulski, N. Gulia and S. Szafert, *Chem. – Eur. J.*, 2015, **21**, 17769–17778.
27 A. Bondi, *J. Phys. Chem.*, 1964, **68**, 441–451.
28 Y. He, Y.-y. Xie, Y.-c. Wang, X.-m. Bin, D.-c. Hu, H.-s. Wang and Y.-m. Pan, *RSC Adv.*, 2016, **6**, 58988–58993.

29 K. Bowden, I. M. Heilbron, E. R. H. Jones and B. C. L. Weedon, *J. Chem. Soc.*, 1946, 39–45, DOI: 10.1039/JR9460000039.

30 H. Hofmeister, K. Annen, H. Laurent and R. Wiechert, *Angew. Chem., Int. Ed. Engl.*, 1984, **23**, 727–729.

 